Inorg. Chem. **2008**, *47*, 3851−3862

Synthesis, Potentiometric, Kinetic, and NMR Studies of 1,4,7,10-Tetraazacyclododecane-1,7-bis(acetic acid)-4,10-bis(methylenephosphonic acid) (DO2A2P) and its Complexes with Ca(II), Cu(II), Zn(II) and Lanthanide(III) Ions

Ferenc K. Kálmán,[†] Zsolt Baranyai,[†,‡] Imre Tóth,[†] István Bányai,[§] Róbert Király,[†] Ernö Brücher,[†] Silvio Aime,[‡] Xiankai Sun,[||] A. Dean Sherry,[⊥,#] and Zoltán Kovács*[,⊥]

Department of Inorganic and Analytical Chemistry and Department of Colloid and Environmental Chemistry, University of Debrecen, P.O. Box 21, Egyetem tér 1, Debrecen H-4010, Hungary, Dipartimento di Chimica I. F. M., Università di Torino, Via P. Giuria 7, I-10125 Torino, Italy, Department of Radiology and Advanced Imaging Research Center, University of Texas Southwestern Medical Center, 5323 Harry Hines Blvd, Dallas, Texas 75390-8568, and Department of Chemistry, University of Texas at Dallas, P.O. Box 830688, Richardson, Texas 75083-0688

Received December 20, 2007

A cyclen-based ligand containing *trans*-acetate and *trans*-methylenephosphonate pendant groups, H_6DO2A2P, was synthesized and its protonation constants (12.6, 11.43, 5.95, 6.15, 2.88, and 2.77) were determined by pH-potentiometry and ^{1}H NMR spectroscopy. The first two protonations were shown to occur at the two macrocyclic ring N–CH_2–PO_3^{2-} nitrogens while the third and fourth protonations occur at the two phosphonate groups. In parallel with protonation of the two $-PO_3^{2-}$ groups, the protons from the $NH^+-CH_2-PO_3^{2-}$ are transferred to the $N-CH_2-COO^-$ nitrogens. The stability constants of the Ca^{2+}, Cu^{2+}, and Zn^{2+} (ML, MHL, MH_2L, and M_2L) complexes were determined by direct pH-potentiometry. Lanthanide(III) ions (Ln^{3+}) form similar species, but the formation of complexes is slow; so, "out-of-cell" pH-potentiometry (La^{3+}, Eu^{3+}, Gd^{3+}, Y^{3+}) and competitive spectrophotometry with Cu(II) ion (Lu^{3+}) were used to determine the stability constants. By comparing the log K_{ML} values with those of the corresponding DOTA (H_4DOTA = 1,4,7,10-tetraazacyclododecane-1,4,7,10-tetraacetic acid) and DOTP (H_8DOTP = 1,4,7,10-tetraazacyclododecane-1,4,7,10-tetramethylenephosphonic acid) complexes, the order DOTA < DO2A2P < DOTP was found for all the metal ion complexes examined here with the exception of the Ca^{2+} complexes, for which the order is reversed. The relaxivity of Gd(DO2A2P) decreases between pH 2 and 7 but remains constant in the pH range of 7 < pH < 12 (r_1 = 3.6 mM^{-1} s^{-1}). The linewiths of the ^{17}O NMR signals of water in the absence and presence of Gd(DO2A2P) (at pH = 3.45 and 8.5) between 274 and 350 K are practically the same, characteristic of a $q = 0$ complex. Detailed kinetic studies of the Ce^{3+} and Gd^{3+} complexes with DO2A2P showed that complex formation is slow and involves a high stability diprotonated intermediate Ln(H_2DO2A2P)*. Rearrangement of the diprotonated intermediate into the final complex is an OH^- assisted process but, unlike formation of Ln(DOTA) complexes, rearrangement of Ln(H_2DO2A2P)* also takes place spontaneously likely as a result of transfer of one of the protons from a ring nitrogen to a phosphonate group. The order of the OH^- assisted formation rates of complexes is DOTA > DO2A2P > DOTP while the order of the proton assisted dissociation rates of the Gd^{3+} complexes is reversed, DOTP > DO2A2P > DOTA. ^{1}H and ^{13}C NMR spectra of Eu(DO2A2P) and Lu(DO2A2P) were assigned using two-dimensional correlation spectroscopy (2D COSY), heteronuclear multiple quantum coherence (HMQC), heteronuclear chemical shift correlation (HETCOR), and exchange spectroscopy (EXSY) NMR methods. Two sets of ^{1}H NMR signals were observed for Eu(DO2A2P) characteristic of the presence of two coordination isomers in solution, a twisted square antiprism (TSAP) and a square antiprism (SAP), in the ratio of 93% and 7%, respectively. Line shape analysis of the ^{1}H NMR spectra of Lu(DO2A2P) gave lower activation parameters compared to La(DOTP) for interconversion between coordination isomers. This indicates that the Ln(DO2A2P) complexes are less rigid probably due to the different size and spatial requirements of the carboxylate and phosphonate groups.

Introduction

Complexes of lanthanides formed with the cyclen derivative DOTA (H_4DOTA = 1,4,7,10-tetraazacyclododecane-1,4,7,10-tetraacetic acid) are widely used in different fields of medical diagnosis and therapy due to their high thermo-

* To whom correspondence should be addressed. E-mail: zoltan.kovacs@utsouthwestern.edu.
[†] Department of Inorganic and Analytical Chemistry, University of Debrecen.
[‡] Università di Torino.
[§] Department of Colloid and Environmental Chemistry, University of Debrecen.
[||] Department of Radiology, University of Texas Southwestern Medical Center.
[⊥] Advanced Imaging Research Center, University of Texas Southwestern Medical Center.
[#] University of Texas at Dallas.

10.1021/ic7024704 CCC: $40.75
Published on Web 04/02/2008

dynamic and kinetic stabilities.[1–4] These favorable complexation properties are related to the rigid structure of the lanthanide(III) (Ln^{3+}) DOTA complexes in which the Ln^{3+} ion occupies a position in the coordination cage formed by the four ring nitrogens and four carboxylate oxygens. The many advantageous properties of the $Ln(DOTA)^-$ complexes have attracted widespread interest in the synthesis of new DOTA derivatives that may have even more favorable complexation behavior. The macrocyclic 1,4,7,10-tetraazacyclododecane backbone plays an important role in the rigidity of these complexes so it is widely used in the design of new ligands where one or more acetate groups of the DOTA are replaced with some other charged or uncharged pendant arms.[1,2,5,6]

The tetrakis(methylene phosphonate) derivative of cyclen, DOTP (H_8DOTP = 1,4,7,10-tetraazacyclododecane-1,4,7,10-tetramethylenephosphonic acid) was reported soon after DOTA.[7,8] The protonation and complexation behavior of DOTP and the relaxation properties of its Gd^{3+} complex have been studied in detail.[9–17] While the stability constants of the $Ln(DOTP)^{5-}$ complexes are higher than those of the corresponding $Ln(DOTA)^-$ complexes, potential biomedical applications of DOTP are more limited than DOTA partly because of the high negative charge on the $Ln(H_nDOTP)^{(5-n)-}$ (n = 1, 2, 3, and 4) complexes over the pH range 3–9.[13] $Gd(HDOTP)^{4-}$ exists largely as a monoprotonated species near pH 7, so the high negative charge of this complex plus the absence of an inner-sphere water molecule[16–18] gives $Gd(HDOTP)^{4-}$ no particular advantage over $Gd(DOTA)^-$ as a contrast agent for magnetic resonance imaging. However, $Tm(HDOTP)^{4-}$ has been shown to induce large paramagnetic shifts in ion-paired, NMR active cations so it has proven useful as a ^{7}Li, ^{23}Na, or ^{39}K NMR shift reagent in isolated cells, perfused tissues, and intact animals.[19–21] $Gd(HDOTP)^{4-}$ has a larger effect on the relaxation rates of water protons than expected for a $q = 0$ complex. This has been interpreted as due to the formation of strong H-bonds in the second sphere between the phosphonate oxygens and the surrounding water molecules.[18] A few alkyl/aryl phosphinate and phosphonate monoester derivatives of DOTP have also been reported. Compared to DOTP, the stability constants of the Ln^{3+} complexes of these ligands are much lower but the kinetic stabilities are somewhat higher.[14,22] The presence of the alkyl or aryl phosponate groups render these ligands and their complexes significantly more hydrophobic than $Ln(HDOTP)^{4-}$.[23]

More recently, some new DOTA derivatives have been prepared in which one, two, and three carboxylate groups were replaced with phosphonates. Taborsky et al. synthesized the triacetate-monophosphonate derivative (DO3AP) and reported its complexation properties.[24] We synthesized the bis(acetate)-bis(methylene phosphonate) (DO2A2P) and mono(acetate)-tris(methylene phosphonate) (DO3PA) derivatives, and while that work was in progress, Lacerda et al. independently reported the synthesis of DO2A2P and examined some potential nuclear medicine applications of this ligand with ^{153}Sm(III) and ^{166}Ho(III).[25] The availability of DO3AP, DO2A2P, and DO3PA offers the possibility of a systematic study of the complexation properties of cyclen based ligands with mixed pendant arms. In this paper, we discuss the synthesis and complexation properties of the ligand, DO2A2P, the relaxation properties of Gd(DO2A2P), and the solution structures of the Eu^{3+} and Lu^{3+} complexes as determined by multinuclear NMR spectroscopy.

Experimental Details

Synthesis of DO2A2P. Paraformaldehyde (0.47 g, Aldrich) was added to a mixture of 1,7-DO2A-*tert*-butyl ester[26] (3.00 g) and triethyl phosphite (2.86 g, Aldrich), and the mixture was stirred for 4 days at room temperature. The volatile impurities were removed by keeping the mixture in vacuum at 60 °C for 1 day to yield a clear oil (5.15 g) that consisted of the ester intermediate and a small amount of diethyl hydroxymethyl phosphonate. This product was used without further purification in the acid hydrolysis of the ethyl phosphonate and *tert*-butyl carboxylate ester groups. The oil was dissolved in hydrochloric acid (20%, 75 mL), and the

(1) *The Chemistry of Contrast Agents in Medical Magnetic Resonance Imaging*; Merbach, A. E., Tóth, É., Eds.; Wiley: Chichester 2001.
(2) Caravan, P.; Ellison, J. J.; McMurry, T. J.; Lauffer, R. B. *Chem. Rev.* **1999**, *99*, 2293.
(3) Volkert, W. A.; Hoffman, T. J. *Chem. Rev.* **1999**, *99*, 2269.
(4) Rösch, F.; Aronsson, E. F. In *Metal Ions in Biological Systems*; Siegel, A., Siegel, H., Eds.; Marcel and Dekker, Inc.: New York 2004; Vol. *42*, p 77.
(5) Alexander, V. *Chem. Rev.* **1995**, *95*, 273.
(6) Jacques, V.; Desreux, J.-F. In *Chemistry of Contrast Agents in Medical Magnetic Resonance Imaging*; Merbach, A. E., Tóth, É., Eds.; Wiley: Chichester, 2001; p 157.
(7) Kabachnik, I. M.; Medved, T. Ya.; Bel'skii, F. I.; Pisareva, S. A. *Izv. Akad. Nauk SSSR, Ser. Khim.* **1984**, 844.
(8) Sherry, A. D.; Malloy, C. R.; Jeffrey, F. M. H.; Cacheris, W. P.; Geraldes, C. F. G. C. *J. Magn. Reson.* **1988**, *76*, 528.
(9) Geraldes, C. F. G. C.; Sherry, A. D.; Cacheris, W. P. *Inorg. Chem.* **1989**, *28*, 3336.
(10) Lázár, I.; Hrncir, D. C.; Kim, W. D.; Kiefer, G. E.; Sherry, A. D. *Inorg. Chem.,* **1992**, *31*, 4422.
(11) Delgado, R.; Siegfried, L. C.; Kaden, T. A. *Helv. Chim. Acta* **1990**, *73*, 140.
(12) Aime, S.; Botta, M.; Terreno, E.; Anelli, P. L.; Uggeri, F. *Magn. Reson. Med.* **1993**, *30*, 583.
(13) Sherry, A. D.; Ren, J.; Huskens, J.; Brücher, E.; Tóth, É.; Geraldes, C. F. C. G.; Castro, M. M. C. A.; Cacheris, W. P. *Inorg. Chem.* **1996**, *35*, 4604.
(14) Burai, L.; Király, R.; Lázár, I.; Brücher, E. *Eur. J. Inorg. Chem.,* **2001**, 813.
(15) Geraldes, C. F. G. C.; Brown, R. D. III.; Cacheris, W. P.; Koenig, S. H.; Sherry, A. D.; Spiller, M. *Magn. Reson. Med.* **1989**, *9*, 94.
(16) Geraldes, C. F. G. C.; Sherry, A. D.; Kiefer, G. E. *J. Magn. Reson.* **1992**, *97*, 290–304.
(17) Avecilla, F.; Peters, J. A.; Geraldes, C. F. G. C. *Eur. J. Inorg. Chem.* **2003**, 4179.
(18) Botta, M. *Eur. J. Inorg. Chem.* **2000**, 399.
(19) Ramaprasad, S.; Lindquist, D. M.; Wall, P. T. *J. Environ. Sci. Heal. A* **1999**, *A34*, 1839–1848.
(20) Winter, P. M.; Seshan, V.; Makos, J. D.; Sherry, A. D.; Malloy, C. R.; Bansal, N. *J. Appl. Physiol.* **1998**, *85*, 1806–1812.
(21) Radford, N. B.; Babcock, E. E.; Richman, A.; Szczepaniak, L.; Malloy, C. R.; Sherry, A. D. *Magn. Reson. Med.* **1998**, *40*, 544–550.
(22) Kim, W. D.; Kiefer, G. E.; Huskens, J.; Sherry, A. D. *Inorg. Chem.* **1997**, *36*, 4128.
(23) Aime, S.; Batsanov, A. S.; Botta, M.; Dickins, R. S.; Faulkner, S.; Foster, C. E.; Harrison, A.; Howard, J. A. K.; Moloney, J. M.; Norman, T. J.; Parker, D.; Royle, L.; Williams, J. A. G. *Chem. Soc. Dalton Trans.* **1997**, 3623–3636.
(24) Taborsky, P.; Lubal, P.; Havel, J.; Kotek, J.; Hermann, P.; Lukes, I. *Collect. Czech. Chem. Commun.* **2005**, *70*, 1909.
(25) Lacerda, S.; Campello, M. P.; Marques, F.; Gano, L.; Santos, I. In *Metal Ions in Biology and Medicine*; Alpoim, M. C., Morais, P. V., Santos, M. A., Cristovao, A. J., Centeno, J. A., Collery, P., Eds.; John Libbey Eurotext: Paris , 2006; Vol. *9*, p 46.
(26) Kovács, Z.; Sherry, A. D. *Synthesis* **1997**, 759–763.

solution was refluxed for 2 days. The hydrochloric acid was removed by rotary evaporation, and the residue was redissolved in water (75 mL), treated with activated carbon (1 g), filtered, and evaporated again by rotary evaporation. The residue was redissolved in a small amount of water (5 mL), and ethanol (50 mL) was added in small portions. A white amorphous solid precipitated. The solution was decanted, and the residue was redissolved in water (5 mL) and stirred for 24 h, over which period the product separated as a white crystalline solid. The solid was filtered, washed with water (2 × 3 mL), and dried in air to give 2.38 g (66.6%) of product. Anal. calcd for $C_{14}H_{30}N_4O_{10}P_2$: C, 35.30; H, 6.35; N, 11.76. Found: C, 35.27; H, 6.46; N, 11.58. ^{1}H NMR (400 MHz, D_2O, ND_3, pD ~ 9–10) δ = 3.31 (8H, s br, N*CH*$_2$ ring), 3.16 (4H, s, *CH*$_2$COOH), 2.94–2.92 (8H, m br, N*CH*$_2$ ring), 2.85 (4H, d, J_{H-P} = 11.2 Hz *CH*$_2$PO$_3$H$_2$). ^{13}C NMR (100 MHz, D_2O, ND_3, pD ~ 9–10) δ = 179.13 (COOH), 57.44 (N*CH*$_2$COOH), 51.57 (N*CH*$_2$ ring), 50.49 (N*CH*$_2$PO$_3$H$_2$, J_{C-P} = 126.41 Hz), 49.66 (N*CH*$_2$ ring). ^{31}P NMR (161 MHz, D_2O, ND_3, pD ~ 9–10) δ = 6.24. MALDI-TOF: *m*/*z*, 477.6 (100% $[M + H]^+$).

Equilibrium Measurements. The chemicals used in the experiments were of the highest analytical grade. For the preparation of the $LnCl_3$ solutions, Ln_2O_3 (Fluka, 99.9%) was dissolved in 6.0 M HCl and the excess acid was evaporated. An aqueous solution of $CeCl_3$ was prepared from $CeCl_3 \cdot 7H_2O$ (Aldrich, 99.9%). The concentration of the $LnCl_3$, $CaCl_2$, $CuCl_2$, and $ZnCl_2$ solutions were determined by complexometric titration with standardized Na_2H_2EDTA and xylenol orange ($LnCl_3$), murexide ($CuCl_2$, $ZnCl_2$), and Patton & Reeder ($CaCl_2$) as indicator. The concentration of DO2A2P was determined by pH-potentiometric titration in the presence and absence of a large (40-fold) excess of $CaCl_2$.

The protonation constants of DO2A2P and the stability constants of the complexes formed with Ca^{2+}, Cu^{2+}, and Zn^{2+} have been determined by pH-potentiometric titration. The metal/ligand concentration ratios were 1:1 and 2:1 (the concentration of the ligand was generally 2.0 mM). Due to slow complex formation, the stability constants of the Ln(DO2A2P) complexes were determined by use of an "out-of-cell" technique as follows. Nine Ln^{3+}(2 mM)−DO2A2P (2 mM) samples (1.5 mL) were prepared with pH values in the pH range about 1.8–3.8 (depending on the Ln^{3+}) at equilibrium. The samples contained 1.0 M KCl to maintain constant ionic strength. The samples were sealed from air maintained at 50 °C for 3 weeks followed by an additional 1 week at 25 °C to reach equilibrium. In the case of Lu(DO2A2P), a competition reaction was used to determine the stability constant because of solubility problems. Nine samples were prepared containing Cu^{2+} (0.1 mM), DO2A2P (0.1 mM), and Lu^{3+} of different concentrations, and after reaching equilibrium, the pH and the absorbance of the samples were measured. The absorbance values were determined at nine different wavelengths between 310 and 350 nm. The molar absorptivity of Cu(DO2A2P) was determined in a separate experiment. In addition to the protonation constants of the ligand, the protonation constants of the complexes determined in separate titration experiments were also used in the calculation of the stability constants of Ln(DO2A2P) complexes.

The pH measurements and titrations were performed in the pH range 1.7–12.5 with a Radiometer PHM93 pH meter, an ABU 80 autoburette, and a Metrohm 6.0234.100 combined electrode. The stirred samples (15 mL) were thermostatted at 25 °C, and the titrations were performed under an inert gas atmosphere by bubbling Ar across the solutions. KH-phthalate (pH = 4.005) and borax (pH = 9.180) buffers were used to calibrate the pH meter. A 0.01 M HCl solution (1.0 M for KCl) was titrated with standardized KOH solution. The differences between the measured and calculated pH values were used to calculate the H^+ concentrations from the experimentally measured pH values as described by Irving et al.[27] The ion product of water was determined from the same HCl−KOH titration experiments over the pH range of about 11–12 (pK_w = 13.83).

The protonation and stability constants were evaluated from the titration data using the program PSEQUAD.[28] For the calculation of the stability constant of Lu(DO2A2P), in addition to the concentrations and pH values, the measured absorbances and the molar absorptivity values of Cu(DO2A2P) were also taken into account.

Relaxation Rates. The longitudinal water proton relaxation times (T_1) were measured using a Stelar Spinmaster (Mede, Pavia, Italy) spectrometer operating at 0.47 T and a standard inversion–recovery sequence. A typical 90° pulse width was 3.5 μs, and the reproducibility of the T_1 data was ±0.5%. The temperature was controlled with a Stelar VTC-91 air-flow heater equipped with a copper−constantan thermocouple (uncertainty ±0.1 °C).

Kinetic Studies. The rate of formation of Ce(DO2A2P) was studied in 1.0 M KCl by spectrophotometry at 312 nm in a thermostatted cell holder (25 °C) using a Cary 1E spectrophotometer. The concentration of the Ce^{3+} was 4×10^{-4} M, and DO2A2P was used in 5−20-fold excess. MES buffer (0.05 M) was used to keep the pH constant. The absorbance values measured at different t time intervals were fitted to eq 1 for the calculation of the first order rate constants (k_{obs} or k_p):

$$k_p = \frac{1}{t} \ln \frac{(A_o - A_e)}{(A_t - A_e)} \quad (1)$$

where A_0, A_t, and A_e are the absorbance values measured at the start of the reaction, at time t, and at equilibrium, respectively.

The formation and dissociation rates of Gd(DO2A2P) were studied by relaxometry at 25 °C with an MS-4 NMR spectrometer (Institute Jozef Stefan, Ljubljana) at 9 MHz. The temperature of the sample holder was controlled with thermostatted air. The longitudinal relaxation times were measured by the "inversion–recovery" method (180°−τ−90°) using 6–8 different τ values, and the sample relaxivity was determined from these data by dividing by the solution concentration in millimolar. Complex formation was studied for a mixture of 1.0 mM Gd^{3+} and 20 mM DO2A2P solutions at different pH values (5.3 < pH < 6.5), a condition that insures complete formation of the intermediate species, Gd(DO2A2P)*.

The acid assisted dissociation rate of Gd(DO2A2P) was determined in 0.1–1.0 M HCl at constant ionic strengh ([HCl] + [KCl] = 1.0 M) at 25 °C. The first order rate constants (k_{obs} or k_p) were calculated using eq 1 except that instead of the absorbance values A_0, A_t, and A_e, relaxivities measured at the start of the reaction (r_{10}), at time t (r_{1t}), and at equilibrium (r_{1e}) were used in the fitting. The relaxivities were obtained from the relaxation times, $r_1 = 1/T_{1m} - 1/T_{1w}$, where T_{1m} and T_{1w} are the water proton longitudinal relaxation times measured in the presence and absence of Gd^{3+}, respectively.

^{17}O NMR. Variable temperature ^{17}O NMR measurements were performed on nonspinning samples at 14.1 T using a Bruker Avance 600 spectrometer. A capillary filled with D_2O was used as an external lock. Experimental settings were as follows: spectral width 10 000 Hz, 90° pulse (7 μs), acquisition time 10 ms, 1000 scans.

(27) Irving, H. M.; Miles, M. G.; Pettit, L. D. *Anal. Chim. Acta* **1967**, *38*, 475.
(28) Zékány, L.; Nagypál, I. In *Computional Methods for Determination of Formation Constants*; Legett, D. J., Ed.; Plenum: New York, 1985; p 291.

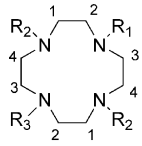

R_1, R_2, R_3 = CH_2COOH: **H_4DOTA**

R_1, R_2, R_3 = $CH_2PO_3H_2$: **H_8DOTP**

R_1, R_3 = $CH_2PO_3H_2$; R_2 = H: **H_4DO2P**

R_1, R_3 = $CH_2PO_3H_2$; R_3 = CH_2COOH: **H_6DO2A2P**

R_1, R_2, = CH_2COOH; R_3 = $CH_2PO_3H_2$: **H_5DO3AP**

R_1 = CH_2COOH; R_2, R_3 = $CH_2PO_3H_2$: **H_7DO3PA**

Figure 1. Structures of the ligands and the numbering of the ring carbon atoms.

The samples contained water enriched to 2.6% ^{17}O (Yeda, Israel). The half-height line width of the ^{17}O NMR signal ($\Delta\nu_{1/2}$) was determined in the presence and absence of Gd(DO2A2P) (5.42×10^{-2} M, 1.0 M KCl).

NMR Experiments. The ^1H and ^{31}P NMR chemical shifts of DO2A2P were determined as a function of pH to evaluate some of the protonation constants. A 0.01 M solution of the ligand in H_2O with 10% D_2O was prepared. The pH was adjusted by stepwise addition of a solution of KOH and HCl (both prepared in H_2O). The protonation constants were determined by fitting of the chemical shift versus pH data using Micromath Scientist, version 2.0 (Salt Lake City, UT).

NMR spectra of some metal ion complexes of DO2A2P were measured in 0.07 M samples prepared in D_2O. ^1H, ^{13}C, and ^{31}P NMR spectra were collected using either a JEOL EX-400 (9.4 T) or Bruker DRX 360 NMR spectrometer. Variable temperarture ^{13}C NMR measurements were carried out using a Bruker DRX 360 NMR spectrometer equipped with Bruker VT-1000 thermocontroller. The ^{31}P NMR spectra of the Eu(DO2A2P) complex were recorded using frequency-selective ^1H decoupling. The chemical shifts are reported in ppm, relative to TMS for ^1H and ^{13}C and H_3PO_4 for ^{31}P as the external standard. The H−H correlation spectroscopy (COSY) and exchange spectroscopy (EXSY) spectras were collected by using gradient pulses in the z direction with the standard JEOL pluse program (in the case of EXSY spectra, the mixing time (τ_M) was 10 ms.) The H−C correlation spectrum was recorded on JEOL EX-400 spectrometer in inverse mode by using gradient pulses in the z direction with the usual JEOL heteronuclear multiple quantum coherence (HMQC) pulse sequence.

Results and Discussion

Synthesis of DO2A2P. DO2A2P (Figure 1) was synthesized in good yields by reacting the *tert*-butyl ester of 1,4,7,10-tetraazacyclododecane-1,7-bis(acetic acid)[26] with paraformaldehyde and triethyl phosphite in a Michaelis−Arbuzov type reaction. This method appears to work well for the synthesis of methylenephosphonate derivatives of cyclen.[29] The final product crystallized from an aqueous solution as a zwitterion as shown by elemental analysis. The molecular structure and purity were also confirmed by ^1H, ^{13}C, and ^{31}P NMR and MALDI-TOF mass spectrometry.

pH-Potentiometric Studies. The ligand H_6DO2A2P (H_6L) has two acetate and two methylenephosphonate pendant arms, and so, its properties are expected to be similar to DOTA and DOTP (the charges of the ligands and complexes will be indicated only when necessary). Since the first two protonation constants in DOTA and DOTP are quite high, one would anticipate that DO2A2P would also have two high protonation constants characteristic of two macrocyclic ring nitrogen protonations. The protonation constants, log K_i^H ($K_i^H = [H_iL]/[H_{i-1}L][H^+]$) were calculated from the pH-potentiometric titration data (Table 1). The log K_1^H value is high, but it could be calculated from the pH-potentiometric data because the titration was performed up to pH = 12.5, where the formation of the fully deprotonated ligand L^{6-} was close to 50%. At such high pH values, the ligand $DO2A2P^{6-}$ probably forms complexes with K^+ ions and so the log K_1^H would have been even higher if Me_4NCl had been used to maintain constant ionic strength. Analogous to DOTA and DOTP,[9,30] protonation of *trans*-ring nitrogens is expected to occur first followed by the protonation of the phosphonate groups by the third and fourth protons and the carboxylates by the fifth and sixth protons. The log K_3^H and log K_4^H values are associated with the protonation of the phosphonate groups while the log K_5^H and log K_6^H characterize the protonation of the two carboxylates. These protonation constants are so-called "macroscopic" constants, which can be used in the description of protonation and complexation equilibria.[31] To obtain more information on the sites of protonation, ^1H and ^{31}P NMR spectra of the ligand were also recorded as a function of pH. The ring methylene protons of DO2A2P give rise to two well resolved triplet signals in the entire pH range investigated. The signals of the methylenephosphonate and acetate methylene protons were doublet and singlet, respectively. The ^{31}P signal of the phosphonate group was broad in the entire pH range. The chemical shifts of the ^1H and ^{31}P signals as a function of pH are presented in Figure 2.

Table 1. Protonation Constants of the Ligands DO2A2P, DOTA, and DOTP (25 °C)

	DO2A2P	DOTP[a]	DOTA[b]
	1.0 M KCl	0.1 M $Me_4N(NO_3)$	0.1 M Me_4NCl
log K_1^H	12.6 (0.01)	13.7[c]	12.6
log K_2^H	11.43 (0.01)	12.2[c]	9.70
log K_3^H	5.95 (0.01)	9.28	4.50
log K_4^H	6.15 (0.01)	8.09	4.14
log K_5^H	2.88 (0.01)	6.12	2.32
log K_6^H	2.77 (0.01)	5.22	

[a] Reference 13. [b] Reference 32. [c] Determined by ^1H NMR titration without control of the ionic strength.

In the pH-range 13.5–10, addition of two equivalents of acid to $DO2A2P^{6-}$ brought about a significant downfield shift of both the ^{31}P and the proton signal of the $CH_2-N-CH_2-PO_3^{2-}$ ring methylene groups indicating that the first two protons are attached to the $N-CH_2-PO_3^{2-}$ ring nitrogens. The protonation of these nitrogens results in the formation of strong H-bonds between the NH^+ and the PO_3^{2-} groups, which explains the high values of log K_1^H and log K_2^H. The proton signals of the acetate methylene protons were also shifted, which is interpreted by the dissociation of the

(29) Burai, L.; Ren, J.; Kovács, Z.; Brücher, E.; Sherry, A. D. *Inorg. Chem.* **1998**, *37*, 69–75.

(30) Desreux, J. F.; Merciny, E.; Loncin, M. F. *Inorg. Chem.* **1981**, *20*, 987.

(31) Beck, M. T.; Nagypál, I. *Chemistry of Complex Equilibria*; Akadémiai Kiadó: Budapest, 1990.

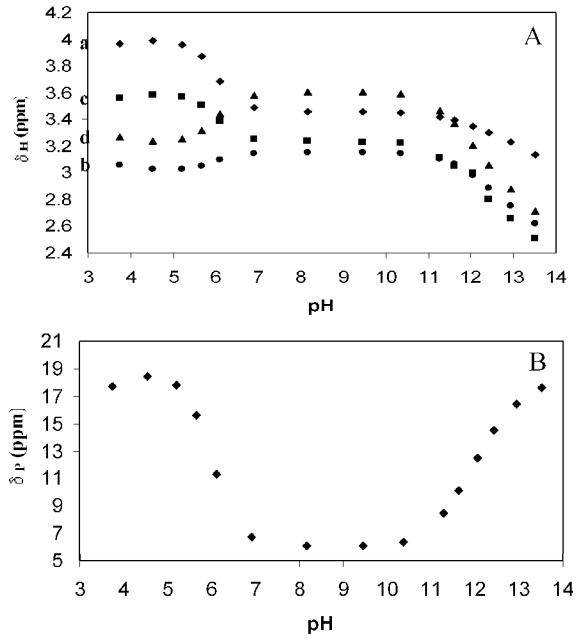

Figure 2. ^{1}H- (A) and ^{31}P NMR chemical shifts (B) of DO2A2P as a function of pH. (A) N−*CH*$_2$−COO$^-$ (a); N−*CH*$_2$−PO$_3^{2-}$ (b, center of the doublet); *CH*$_2$−N−CH$_2$−COO$^-$ (c); *CH*$_2$−N−CH$_2$−PO$_3^{2-}$ (d).

complex K$^+$−DO2A2P^{6-} formed at higher pH values. Similar ^{1}H and ^{31}P NMR shifts have been observed during the titration of H_8DOTP with Me_4NOH and NaOH when Na$^+$−DOTP^{8-} complexes were formed.[9]

In the pH interval about 10–7, there is practically no change in the chemical shift values (Figure 2). Further lowering of the pH resulted in the strong downfield shift of the ^{31}P signal between pH 7 and 5, confirming that the log K_3^H and log K_4^H values are related to the protonation of the phosphonate groups. However, in this same pH range the signals of the N−*CH*$_2$−PO$_3$ and *CH*$_2$−N−CH$_2$−PO$_3$ methylene protons shifted to lower frequencies (upfield). These findings can be explained by assuming that parallel with the protonation of the PO$_3^{2-}$ groups the protons from the NH$^+$−CH$_2$−PO$_3^{2-}$ nitrogens are transferred to the N−CH$_2$−COO$^-$ nitrogens, which also result in a strong downfield shift of the signal of the acetate methylene protons. (Figure 2A). At pH values below 4, the carboxylate groups of the ligand start to be protonated. The protonation constants log K_3^H and log K_4^H are much lower than those for the DOTP (Table 1) probably because for the protonation of the phosphonate groups to occur, the first two protons must be transferred from the NH$^+$−CH$_2$−PO$_3^{2-}$ nitrogens to the N−CH$_2$−COO$^-$ nitrogens. This proton transfer is not favorable as the H-bonds between the protonated nitrogens and PO$_3^{2-}$ groups are strong. Calculation of the first four protonation constants from the ^{1}H NMR chemical shift data in the pH range 3.7–13.5 gave log $K_1^H = 12.8$, log $K_2^H = 11.7$, log $K_3^H = 5.93$, and log $K_4^H = 6.25$. The first two protonation constants are somewhat higher than those obtained by pH-potentiometry (Table 1), probably because the solution samples used for the ^{1}H NMR titration experiments did not contain KCl to keep the ionic strength constant. The value obtained from the ^{1}H NMR study for third and fourth protonation agrees well with the potentiometric data but, surprisingly, both the NMR and potentiometric log K_4^H is larger than log K_3^H, which is the opposite of the usual decreasing order of protonation constants. This unexpected finding is probably due to the peculiar structure of the triprotonated ligand H_3DO2A2P^{3-}. Interpretation of the ^{1}H NMR chemical shifts suggests that in the triprotonated species one phosphonate and two neighboring (cis) nitrogens are protonated. Due to the electrostatic repulsion between these two protonated nitrogens the stability (and consequently the concentration) of this intermediate is low. The attachment of the fourth proton is favorable since it leads to the formation of the symmetric, more stable tetraprotonated species H_4DO2A2P^{2-}. This cooperativity in the protonation steps reverses the expected order of protonation constants.

Table 2. Stability and Protonation Constants of the Complexes of DO2A2P (25 °C, 1.0 M KCl), DOTA, and DOTP

	ML	MHL	MH_2L	M_2L	ML[b]	ML[c]
Ca^{2+}	15.1 (0.07)	7.33 (0.01)	6.40 (0.04)	3.05 (0.07)	17.2[d]	10.3[g]
Cu^{2+}	24.9 (0.04)[a]	6.79 (0.05)	6.30 (0.03)	4.72 (0.04)	22.2[e]	25.4[h]
Zn^{2+}	22.5 (0.03)	6.92 (0.03)	6.34 (0.01)	3.47 (0.08)	21.1[e]	24.8[h]
La^{3+}	23.3 (0.08)	5.40 (0.08)	4.49 (0.08)	2.77 (0.05)	22.9[f]	27.6[i]
Eu^{3+}	25.6 (0.04)	5.34 (0.05)	4.64 (0.05)	3.78 (0.07)	24.7[f]	28.1[i]
Gd^{3+}	25.7 (0.09)	5.32 (0.08)	4.55 (0.08)	3.75 (0.07)	24.7[f]	28.8[i]
Y^{3+}	26.6 (0.09)	5.19 (0.09)	4.27 (0.09)	3.10 (0.05)		
Lu^{3+}	26.4 (0.09)[a]	5.26 (0.02)	4.42 (0.02)	4.33 (0.04)	25.4[f]	29.6[i]

[a] Obtained by spectrophotometry. [b] DOTA. [c] DOTP. [d] Reference 33. [e] Reference 34. [f] Reference 35. [g] Reference 7. [h] Reference 36. [i] Reference 13.

Stability Constants of Complexes. Complex formation equilibria of DO2A2P were studied with Ca^{2+}, Cu^{2+}, Zn^{2+}, and Ln^{3+} ions. The stability (K_{ML}, K_{M2L}) and protonation constants (K_{MHiL}) of the complexes have been defined by eqs 2−4 (the charges of the species are omitted for simplicity).

$$K_{ML} = \frac{[ML]}{[M][L]} \tag{2}$$

$$K_{MH_iL} = \frac{[MH_iL]}{[MH_{i-1}L][H^+]} \tag{3}$$

$$K_{M2L} = \frac{[M_2L]}{[ML][M]} \tag{4}$$

The complexation reactions between DO2A2P and Ca^{2+}, Cu^{2+}, or Zn^{2+} were fast enough to determine the equilibrium constants of eqs 2−4 in direct titration experiments. On the other hand, the formation reactions of the Ln(DO2A2P) complexes were slow and the stability constants (log K_{ML}) were determined by the out-of-cell method. The log K_{MHiL} and log K_{M2L} values have been determined by direct titration of the acidified complex solutions prepared before the measurements. The protonation constants K_{MHL} and K_{MH2L}, determined in the separate experiments, were taken into account in the calculation of the log K_{ML} stability constants of the complexes Ln(DO2A2P). The obtained equilibrium constants of eqs 2−4 are presented in Table 2.

Generally, the stabilities of DOTP complexes is higher than those of DOTA complexes, with the exception of Ca−DOTP, whose stability is much lower than that of Ca−DOTA. As expected, the stability constants of the

DO2AP complexes ML were found to be between the log K_{ML} values of the complexes of DOTA and DOTP. This is also true for the complexes of Ca^{2+}, but in this case the order of log K_{ML} values is Ca(DOTA) > Ca(DO2A2P) > Ca(DOTP). Thus, with the exeption of the Ca^{2+}, which prefers the carboxylate groups over the phosphonates, the replacement of two carboxylates of DOTA with two phosphonate groups leads to an increase in the stability of the complexes.

Similar results were found for the Ln^{3+} complexes of the monophosphonate derivative of DOTA (DO3AP) by Taborsky et al.[24] (The stability constants of the Ln(DO3AP) complexes determined by Taborsky in 0.1 M Me_4NCl are somewhat higher than those of the Ln(DO2A2P) complexes measured by us in 1.0 M KCl. This probably reflects the effect of K(DO2A2P) formation as under identical conditions the opposite order of stabilities is expected.) The stabiliy constants of the Ln(DO2A2P) complexes, similarly to the Ln-complexes of DOTA, DO3AP, and DOTP, slightly increase with decreasing ionic size of lanthanides (Table 2).[24]

The protonation of the M(DO2A2P) complexes probably occurs at the phosphonate or carboxylate groups in the same way as the protonation of $Ln(DOTP)^{5-}$ or $Ln(DOTA)^{-}$ complexes.[13,32] The protonation of the ring nitrogens is not likely, particularly for the Cu^{2+} and Zn^{2+} complex. Surprisingly, the first and second protonation constants log K_{MHL} and log K_{MH2L} of the $Ca^{2+}-$, $Cu^{2+}-$, and $Zn^{2+}-$DO2A2P complexes are higher than the log K_3^H and log K_4^H protonation constants of the phosphonate groups of the free ligand. This interesting observation can be interpreted by assuming the presence of uncoordinated pendant arms in these complexes due to the lower coordination number of Cu^{2+} and Zn^{2+}. Interestingly, the stability constant of the Zn(DO2A2P) is very similar to the that of the Zn^{2+} complex of 1,4,7,10-tetraazacyclododecane-1,7-bis(methylenephosphonic acid) (DO2P) (log $K_{Zn(DO2P)} = 21.2$)[29]], a ligand similar to DO2A2P except lacking the two acetate pendant arms. The nearly identical stability of the $Zn^{2+}-$complexes suggest that the carboxylates do not play a significant role in the formation of Zn(DO2A2P). Unlike the free diprotonated ligands, H-bond formation between the ring nitrogens and phosphonate groups is not possible in the Cu(DO2A2P) and Zn(DO2A2P) complexes, so protonation of these complexes at the phosphonates may take place at higher pH values. For the complexes of lanthanides, where all donor atoms in DO2A2P act as ligands for the metal ion, the log K_{MHL} and log K_{MH2L} values are lower than the log K_3^H and log K_4^H protonation constants of the ligand. This indicates the coordinated phosphonate groups can be protonated in these complexes. The third protonation constants of the Cu^{2+} and Zn^{2+} complexes are low (2.46 and 1.96, respectively), so these must reflect protonation of the carboxylate groups. The stability constants of the dinuclear complexes formed with Zn^{2+}, Cu^{2+}, and Ln^{3+} ions are fairly similar (Table 2) probably because electrostatic interactions predominate in the formation of these complexes.

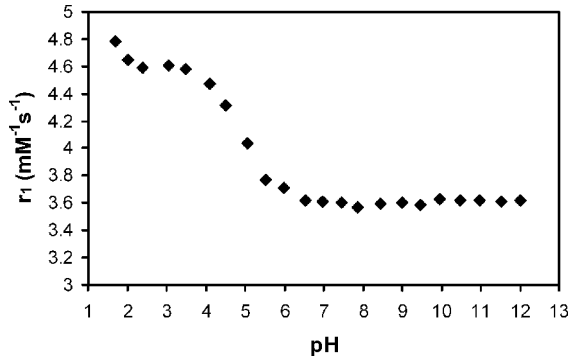

Figure 3. Relaxivity values of Gd(DO2A2P) at 25 °C.

Relaxation Properties of Gd(DO2A2P). The relaxivity of Gd(DO2A2P) as a function of pH at 20 MHz is shown in Figure 3. Protonated complexes are present in the pH range 2–7 so these contribute to the relaxation rates but at pH values above 7 where the complex is fully deprotonated, the relaxivity is relatively constant at 3.6 ± 0.05 mM^{-1} s^{-1}. This value is most consistent with a $q = 0$ complex with a small outer-sphere contribution to relaxivity, much like that noted for Gd(DOTP) previously. The higher relaxivity of the protonated complexes can be explained by faster proton exchange due to the protonation of the noncoordinated oxygen atoms of the PO_3^{2-} group.

It is known that Gd(DOTA) has one inner-sphere coordinated water molecule while Gd(DOTP) has none.[16–18] The presence of one (or more) water molecule(s) in the inner sphere of the paramagnetic Gd^{3+} results in a broadening in the ^{17}O NMR signal of water via the exchange of the coordinated H_2O with the bulk water.[37] The half-widths ($\Delta\nu_{1/2}$) of the ^{17}O NMR signal have been determined in ^{17}O enriched (2.6%) water in the presence and absence of Gd(DO2A2P) at pH = 3.45 and at pH = 8.5 in the temperature range 273–350 K. The $\Delta\nu_{1/2}$ values (Figure S1, Supporting Information) are virtually identical in the presence and absence of Gd(DO2A2P), showing that the presence of the paramagnetic complex has no effect on the ^{17}O NMR water linewidths. This finding indicates that neither the protonated nor deprotonated Gd(DO2A2P) complexes have an inner-sphere water molecule.

Kinetics of Formation of Ln(DO2A2P) Complexes. The formation of Ce(DO2A2P) and Gd(DO2A2P) complexes below pH 7 were slow enough so that the rates of reactions could be studied by conventional techniques. The rates of formation of Ce(DO2A2P) in the pH range 5.3–6.5 were measured in the presence of both metal and ligand excess to afford pseudo-first-order rate constants (k_{obs}). The plot of k_{obs} values against the DO2A2P or Ce^{3+} concentration

(32) Burai, L.; Fábián, I.; Király, R.; Szilágyi, E.; Brücher, E. *J. Chem. Soc., Dalton Trans.* **1998**, 243.
(33) Delgado, R.; Da Silva, J. J. R. F. *Talanta* **1982**, *72*, 567.
(34) Chaves, S.; Delgado, R.; Da Silva, J. J. R. F. *Talanta* **1992**, *39*, 249.
(35) Cacheris, W. P.; Nickle, S. K.; Sherry, A. D. *Inorg. Chem.* **1987**, *26*, 958.
(36) Martell, A. E.; Smith, R. M. *Critical Stability Constants, Vols. 1–6*; Plenum Press: New York, 1974–1989.
(37) Tóth, É.; Helm, L.; Merbach, A. E. *Top. Curr. Chem.* **2002**, *221*, 61.

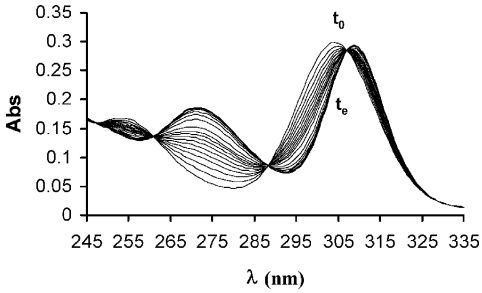

Figure 4. Absorption spectra of the Ce^{3+} + DO2A2P system at the start of the reaction (t_0) and after 100 min, at equilibrium (t_e). ($[Ce^{3+}] = [DO2A2P] = 4 \times 10^{-4}$ M, 25 °C, pH = 5.33).

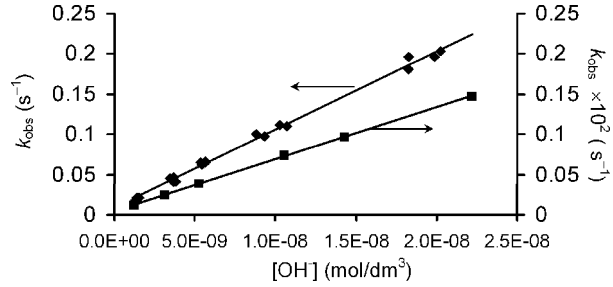

Figure 5. First-order rate constants for the formation reaction of Ce(DO2A2P) (♦) and Gd(DO2A2P) () ($[Ce^{3+}] = 4 \times 10^{-4}$ M, $[DO2A2P] = 8 \times 10^{-3}$ M; $[Gd^{3+}] = 1 \times 10^{-3}$ M, $[DO2A2P] = 1 \times 10^{-2}$ M, 1.0 M KCl, 25 °C).

gave a saturation curve indicating the formation of a intermediate.[38] This was also confirmed by spectrophotometry (Figure 4).

During formation of Ce(DOTA), a diprotonated intermediate, Ce(H_2DOTA)* was detected by spectrophotometry and was shown to have two protonated macrocyclic ring nitrogens (in trans postions) while Ce^{3+} is coordinated only to the carboxylate oxygens.[32,38] We assumed that fast formation of a similar diprotonated intermediate, Ce(H_2DO2A2P)*, might make it possible to measure the stability constant of this species by a direct pH-potentiometric titration. Indeed, titration of a $Ce^{3+}(2 \times 10^{-3}$ M)−DO2A2P(2×10^{-3} M) solution in the pH range 1.8–4.0 gave a stability constant log $K_{CeH2L*} = 10.4$ (0.07) and protonation constant log $K^{H}_{CeH2L*} = 3.9$ (0.03) for this intermediate. During the calculation of the stability constant of Ce(H_2DO2A2P)* lower standard deviation values were obtained by assuming the formation of a triprotonated intermediate as well. It is very likely that the species Ce(H_2DO2A2P)* has a similar structure to Ce(H_2DOTA)* with the Ce^{3+} ion coordinated to two carboxylate oxygens and two phosphonate oxygens. The stability constant of the intermediate Ce(H_2DO2A2P)* is significantly higher than that of Ce(H_2DOTA)* (log $K^{H}_{CeH2L*} = 4.5$[38]), probably due to the participation of the phosphonates in coordination to the metal ion. The stability constant of La(H_2DO2P), where again the protons are located on two macrocyclic nitrogens, is also significantly lower (log $K_{(LaH2L)} = 7.6$)[29] than that of the Ce(H2DO2A2P)*. These data strongly suggest that both the phosphonate and carboxylate groups are coordinated in the Ce(H2DO2A2P)* intermediate. For the formation of Ce(DO2A2P), the Ce^{3+} must displace the two protons from the macrocyclic ring nitrogens before entering the coordination cage of the macrocycle. Since removal of these protons from the very basic ring nitrogens is not favored, formation of the final complex is slow. In the pH range 5.3–6.5, where the formation rates of the complexes were studied, the concentration of the triprotonated intermediate is very low, so its role in the complex formation is probably negligible. This assumption was confirmed by spectrophotometric studies. The presence of isosbestic points in the absorption spectra (Figure 4) indicates the formation of two species, the intermediate Ce(H_2-DO2A2P)* with an absorption maximum at 304 nm and the product, Ce(DO2A2P) showing an absorption maximum at 309 nm.

The rates of formation of Ce(DO2A2P) and Gd(DO2A2P) were studied in the presence of excess ligand ($[L]_t/[Ln^{3+}] = 20$) because the saturation values in the plots of k_{obs} versus $[Ce^{3+}]$ showed a decreasing trend with increasing Ce^{3+} concentration. We assumed that the decrease in k_{obs} observed at high Ce^{3+} concentrations reflected formation of a dinuclear diprotonated intermediate. Ce_2(H_2DO2A2P)*. The stability constants of the dinuclear intermediate [Ce(H_2DO2A2P)$^-$ + Ce^{3+}] was determined by pH-potentiometry in the pH range about 1.8–4.0, exploiting the competition between the H^+ and the excess Ce^{3+} ions for the intermediate, Ce(H_2DO2A2P)*. The stability constant of the dinuclear intermediate, Ce_2(H_2DO2A2P)*, was found to be log $K_{Ce2H2L} = 3.2$ (0.07). To avoid any complications that might arise from the formation of the dinuclear intermediate, all further kinetic studies were performed in the presence of ligand excess. Under pseudofirst-order conditions the formation rate of the Ln(DO2A2P) complexes can be described by

$$\frac{d[LnL]_t}{dt} = k_{obs}[Ln^{3+}] \quad (5)$$

where $[LnL]_t$ is the total concentration of the complex, Ln(DO2A2P). The k_{obs} values obtained at different pH values show a direct proportionality with the increase of the OH^- concentration (Figure 5). Unlike the results obtained for the formation of Ln(DOTA) complexes, the straight line obtained by plotting the k_{obs} values against the $[OH^-]$ has a positive intercept. Similarly, when values of k_{obs} for Gd(DO2A2P) were plotted against the OH^- concentration, that graph also had a positive intercept (Figure 5). Thus, the rate constants, k_{obs}, obtained for the formation reactions of Ce(DO2A2P) and Gd(DO2A2P) can be expressed as:

$$k_{obs} = k_L + k_{OH}[OH^-] \quad (6)$$

where k_{OH} is the rate constant characterizing the transformation of the intermediate Ln(H_2DO2A2P)* to product catalyzed by OH^- while the rate constant, k_L, reflects "spontaneous" transformation of the intermediate to product, Ln(DO2A2P).

The formation of Ln(DO2A2P) complexes by the OH-assisted pathway presumably occurs via mechanism similar to that proposed for the formation of Ln(DOTA)$^-$ com-

(38) Tóth, É.; Brücher, E.; Lázár, I.; Tóth, I. *Inorg. Chem.* **1994**, *33*, 4070.
(39) Kumar, K.; Chang, C. A.; Tweedle, M. F. *Inorg. Chem.* **1993**, *32*, 587.

Table 3. Rate Constants, Characterizing the Formation of the Ce^{3+} and Gd^{3+} Complexes of DOTA, DO3AP, DO2A2P, and DOTP (25 °C)

	DOTA	DO3AP[c]	DO2A2P		DOTP[d]
	k_{OH} (M^{-1} s^{-1})	k_{OH} (M^{-1} s^{-1})	k_L (s^{-1})	k_{OH} (M^{-1} s^{-1})	k_{OH} (M^{-1} s^{-1})
Ce^{3+}	3.5×10^6 [a]	9.6×10^5	$(9.1 \pm 1) \times 10^{-5}$	$(1.7 \pm 0.04) \times 10^5$	
Gd^{3+}	5.9×10^6 [b]	9.0×10^4	$(3.0 \pm 0.3) \times 10^{-5}$	$(6.6 \pm 0.14) \times 10^4$	7.2×10^3

[a] Reference 32. [b] Reference 39. [c] Reference 24. [d] Reference 14.

plexes.[32,38] It is likely that the diprotonated intermediate is in equilibrium with a monoprotonated intermediate:

$$Ln(H_2DO2A2P)^* \rightleftharpoons Ln(HDO2A2P)^* + H^+ \qquad (7)$$

This equilibrium strongly favors $Ln(H_2DO2A2P)^*$ because the protonation constant of $Ln(HDO2A2P)^*$ is large, presumably only somewhat lower than the protonation constant of the monoprotonated ligand $HDO2A2P^{5-}$, log $K_2^H = 11.43$ (Table 1). (In the case of the formation of DOTA complexes, log $K_2^H = 9.70$ and the protonation constant of the intermediate, Ce(HDOTA)*, is log $K^H_{CeHL^*} = 8.64$.[32]) The formation of the product Ln(DO2A2P) can occur via the formation of the monoprotonated intermediate with the rate determining step being the deprotonation of the species $Ln(HDO2A2P)^*$. Thus, the formation rate of the complex Ln(DO2A2P) is directly proportional to the concentration of the intermediate $Ln(HDO2A2P)^*$, which is directly proportional to the $[H^+]^{-1}$ or $[OH^-]$, as predicted by equilibrium (7).[32] The deprotonation of the intermediate may take place with the participation of a general base such as a water molecule. This is the only plausible pathway for the formation of the $Ln(DOTA)^-$ complexes in the absence of other general bases and in this case the rate expression (6) does not contain the term k_L. However, the intermediates $Ln(H_2DO2A2P)^*$ contain two phosphonate groups, which are more basic than the carboxylates of the $Ln(H_2DOTA)^*$ and one of these phosphonate groups may accept a proton transferred from a ring nitrogen of the diprotonated intermediate. This process can lead to a diprotonated intermediate which is protonated at one ring nitrogen and one phosphonate group. Transfer of the proton from the ring nitrogen to a water molecule in the rate determining step yields $Ln(HDO2A2P)^{2-}$, in which a phosphonate group is protonated, and the formation of this complex is independent from the H^+ (or OH^-) concentration. Over the pH intervals investigated here, the complexes exist as nonprotonated Ln(DO2A2P), monoprotonated Ln(HDO2A2P) and diprotonated $Ln(H_2DO2A2P)$ species as expected on the basis of the protonation constants obtained by pH-potentiometric titration (Table 2). The mono and diprotonated complexes are protonated at the phosphonate oxygens, while the other oxygen of the phosphonate groups is coordinated to the Ln ion located in the coordination cage.

A comparison of the k_{OH} values characterizing the formation of the DO2A2P, DOTA, DO3AP, and DOTP complexes of Ce^{3+} and Gd^{3+} (Table 3) clearly indicates that the gradual replacement of the carboxylate groups of DOTA with phosphonate groups results in a decreased rate of complex formation. For the interpretation of these experimental data, we assume that the extent of preorganization of the ligands (or more accurately, the intermediary metal complexes) decreases with increasing number of the phosphonate groups, since the electrostatic repulsion between the PO_3^{2-} groups or between PO_3^{2-} and COO^- groups is larger than that between multiple COO^- groups. The formation rates are directly proportional to the $[OH^-]$ for all the complexes indicating a similar formation mechanism, which is the deprotonation of a ring nitrogen of the monoprotonated intermediate. However, the increase of the number of the phosphonate groups of the ligand results in an increase in the negative charge of the intermediate, which may slow down the rate of the proton loss. In addition, high negative charge of the pendant arm functional groups results in the formation of a more stable intermediate (the Ln^{3+} is coordinated by the donor atoms of the pendant groups) and the rearrangement rate of the intermediary complex to the final product is slower. Such effects have been implicated in the slow formation of the $Ln(DOTP)^{5-}$ complexes.

Kinetics of Dissociation of Gd(DO2A2P). High kinetic inertness of Ln^{3+} chelates is vital for biomedical applications. The kinetic inertness is often characterized by comparisons of acid-catalyzed dissociation rates of complexes. Therefore, the rates of dissociation of Gd(DO2A2P) to free Gd^{3+} in 0.1–1.0 M HCl and constant ionic strength ([HCl] + [KCl] = 1.0 M) were measured by water relaxation. Release of free Gd^{3+} from the complex in acid solution resulted in an increase of the relaxivity (r_1) since $r_{1(Gd3+)} = 17.0$ mM^{-1} s^{-1} while $r_{1(Gd(HxL))} \approx 7$ mM^{-1} s^{-1} at 9 MHz. Equlibrium calculations using the known protonation constants, K_{GdHL} and K_{GdH2L} (Table 2), indicate that the complex is largely in the diprotonated form, $Gd(H_2DO2A2P)$ (GdH_2L), under these experimental conditions. This species likely has two protons associated with the two appended and coordinated phosphonate groups. The proton from a phosphonate group can be transferred to a ring nitrogen, which eventually leads to the dissociation of the complex. The transfer of the proton is very slow because of the electrostatic repulsion between the coordinated Ln^{3+} ion and the proton.

At a given $[H^+]$ the rate of dissociation is directly proportional to the total concentration of the complex, $[GdL]_t$

$$-\frac{[GdL]_t}{dt} = k_d[GdL]_t \qquad (8)$$

where k_d is a pseudofirst-order rate constant, since $[H^+] >> [GdL]_t$. The k_d values were calculated from the relaxivity measurements and a plot of k_d as a function of $[H^+]$ showed weak saturation at high acid concentrations (Figure 6). Dissociation of GdH_2L was assumed to take place both spontaneously and by a proton assisted mechanism through

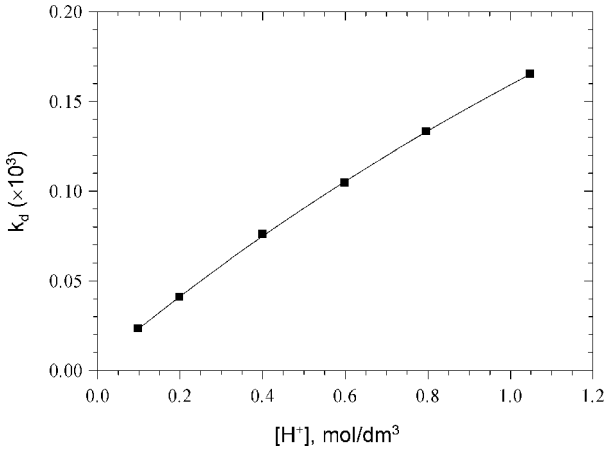

Figure 6. First-order rate constants characterizing the dissociation of Gd(DO2A2P) ([Gd(DO2A2P)] = 1×10^{-3} M, [HCl] + [KCl] = 1.0 M, 25 °C).

formation of a triprotonated species, $Gd(H_3L)$, characterized by the rate constants k_0 and k_1, respectively. The rate of dissociation can be expressed by eq 9:

$$-\frac{d[GdL]_t}{dt} = k_0[GdH_2L] + k_1[GdH_2L][H^+] \qquad (9)$$

Considering that $[GdL]_t = [GdH_2L] + [GdH_3L]$ and the protonation constant $K_{GdH3L} = [GdH_3L]/[GdH_2L][H^+]$, k_d can be expressed from eqs 8 and 9 as follows:

$$k_d = \frac{k_0 + k_1[H^+]}{1 + K_{GdH3L}[H^+]} \qquad (10)$$

The rate constants k_0 and k_1 were obtained by fitting the k_d values to eq 10. These are presented in Table 4 together with the reported values for the Gd(DOTA), Gd(DO3AP), and Gd(DOTP).

From a comparison of these data, it can be concluded that replacement of acetate sidearms of DOTA with methylenephosphonates leads to an increase in the proton-assisted dissociation rate of the Gd^{3+} complexes. This decrease in kinetic inertness likely reflects the mechanism of dissociation. The first step is protonation of an oxygen atom of the coordinated ligand followed by the protonation of a ring nitrogen via an intramolecular proton transfer from a protonated carboxylate or phosphonate. Since it is much easier to protonate a coordinated phosphonate (protonation occurs at pH 5–7) than a carboxylate, the Gd^{3+} complexes containing more phosphonate groups form more stable protonated complexes and therefore transfer of a proton to a ring nitrogen occurs with greater frequency.

^{1}H and ^{13}C NMR Studies of the Ln(DO2A2P) Complexes. The structure of the Ln(DO2A2P) complexes, like many other properties, is expected to be similar to those of the corresponding Ln(DOTA) and Ln(DOTP) complexes. The structure of the Ln(DOTA) complexes has been studied in detail both in the solid state by X-ray diffraction method and in solution by ^{1}H and ^{13}C NMR spectroscopy.[41–50] The structure of different Ln(DOTP) complexes was also studied by several groups.[16,17,51–54] These were found to be quite similar both in solid state and in solution, probably because of the rigid structure of the coordinated DOTA or DOTP ligands. The four ring nitrogens and four carboxylate or phosphonate oxygen donor atoms form two parallel planes and the Ln^{3+} is located between the planes, somewhat closer to the oxygens. The four N and four O donor atoms approximately form a square antiprism. In the case of the Ln(DOTA) complexes, a water molecule is coordinated to the Ln^{3+} ion in a capping position at the center of plane of the four oxygens. The Ln(DOTP) complexes do not contain water molecule in the inner sphere of the Ln^{3+} ion.[17,18]

Because of the rigid structure of the macrocyclic ring, the four ethylene groups adopt identical staggered conformations, which lead to clockwise ($\lambda\lambda\lambda\lambda$) or counterclockwise ($\delta\delta\delta\delta$) helicity of the ring. The acetate groups are accommodated similarly and thus two enantiomers, $\Lambda(\lambda\lambda\lambda\lambda)$ and $\Delta(\delta\delta\delta\delta)$, are formed which give rise to identical NMR spectra. However, the ^{1}H and ^{13}C NMR spectra of several Ln(DOTA) complexes show two sets of signals which have been shown to correspond to two different coordination isomers where the conformation of the macrocyclic ring remains the same but the layout of the acetate sidearms differs.[47–50] For the enantiomer pair $\Lambda(\lambda\lambda\lambda\lambda)$ and $\Delta(\delta\delta\delta\delta)$, the twist angle between the 4N and 4O planes is about 40° corresponding to a square antiprismatic geometry (SAP). Twisting the acetate arms in the opposite direction gives rise to the enantiomer pair $\Lambda(\delta\delta\delta\delta)$ and $\Delta(\lambda\lambda\lambda\lambda)$ having a twist angle of about −30° corresponding to a twisted square antiprismatic geometry (TSAP).[47–50] Ln(DOTP) complexes exist as the TSAP isomer both in solid state and in solution.[17] Both enantiomerization and isomerization of DOTA complexes have been observed by NMR in the temperature range 0 – 100 °C while only enantiomerization was detected in case of the more rigid DOTP complexes.

Ln(DOTA) and Ln(DOTP) complexes have C_4 symmetry and so the ^{1}H and ^{13}C NMR spectra consist of 6 and 4 signals, respectively.[47] The Ln(DO2A2P) complexes how-

(40) Wang, X.; Jin, T.; Comblin, V.; Lopez-Mut, A.; Merciny, E.; Desreux, J. F. *Inorg. Chem.* **1992**, *31*, 1095.
(41) Spirlet, M. R.; Rebizant, J.; Loncin, M. F.; Desreux, J. F. *Inorg. Chem.* **1984**, *23*, 4278–83.
(42) Dubost, J. P.; Leger, J. M.; Langlois, M. H.; Meyer, D.; Schaefer, M. *C. R. Acad Sci. (Paris)* **1991**, *312*, 349–54.
(43) Chang, C. A.; Francesconi, L. C.; Malley, M. F.; Kumar, K.; Gougoutas, J. Z.; Tweedle, M. F.; Lee, D. W.; Wilson, L. J. *Inorg. Chem.* **1993**, *32*, 3501–8.
(44) Parker, D.; Pulukkody, K.; Smith, F. C.; Batsanov, A.; Howard, J. A. K. *J. Chem. Soc., Dalton Trans.* **1994**, 689–93.
(45) Aime, S.; Barge, A.; Botta, M.; Fasano, M.; Ayala, J. D.; Bombieri, G. *Inorg. Chim. Acta* **1996**, *246*, 423–429.
(46) Desreux, J. F. *Inorg. Chem.* **1980**, *19*, 1319–24.
(47) Aime, S.; Botta, M.; Ermondi, G. *Inorg. Chem.* **1992**, *31*, 4291–9.
(48) Hoeft, S.; Roth, K. *Chem. Ber.* **1993**, *126*, 869–73.
(49) Jacques, V.; Desreux, F. *Inorg. Chem.* **1994**, *33*, 4048.
(50) Aime, S.; Botta, M.; Fasano, M.; Marques, M. P. M.; Geraldes, C. F. G. C.; Pubanz, D.; Merbach, A. E. *Inorg. Chem.* **1997**, *36*, 2059–2068.
(51) Geraldes, C. F. G. C.; Brown, R. D., III; Cacheris, W. P.; Koenig, S. H.; Sherry, A. D.; Spiller, M. *Magn. Reson. Med.* **1989**, *9*, 94–104.
(52) Aime, S.; Botta, M.; Parker, D.; Williams, J. A. G. *J. Chem. Soc., Dalton Trans.* **1996**, 17–23.
(53) Sherry, A. D.; Geraldes, C. F. G. C.; Cacheris, W. P. *Inorg. Chim. Acta* **1987**, *139*, 137–9.
(54) Ren, J.; Sherry, A. D. *J. Magn. Reson.* **1996**, *B111*, 178–82.
(55) Aime, S.; Botta, M.; Garino, E.; Crich, S. G.; Giovenzana, G.; Pagliarin, R.; Palmisano, G.; Sisti, M. *Chem.—Eur. J.* **2000**, *6*, 2609–2617.

Table 4. Rate Constants, Characterizing the Dissociation of the Gd^{3+} Complexes of DOTA, DO3AP, DO2A2P, and DOTP (25 °C)

	Gd(DOTA)[a]	Gd(DO3AP)[b]	Gd(DO2A2P)	Gd(DOTP)[c]
k_0 (s^{-1})	$<5 \times 10^{-8}$		$(4.3 \pm 0.5) \times 10^{-6}$	
k_1 (M^{-1} s^{-1})	8.4×10^{-6}	2.78×10^{-3}	$(1.95 \pm 0.04) \times 10^{-4}$	5.4×10^{-4}

[a] Reference 40. [b] Reference 24. [c] Reference 14.

ever have only C_2 symmetry so twelve ^1H resonances and seven ^{13}C NMR resonances were expected and observed experimentally (Figure 7). In the ^1H NMR spectrum, the signals of the two $-CH_2-PO_3^{2-}$ protons overlap at −10.4 ppm and the coupling patterns could not be observed due to the paramagnetism of Eu^{3+}. In the ^{13}C NMR spectrum, however, the signal of the $-CH_2-PO_3^{2-}$ carbon is split into a doublet due to coupling to the ^{31}P nucleus (J_{CP} = 148.8 Hz). The axial (a) and equatorial (e) protons of the ethylene groups are labeled as $_1H_a$, $_1H_e$, $_2H_a$, $_2H_e$, $_3H_a$, $_3H_e$, $_4H_a$, and $_4H_e$ according to the numbering of carbon atoms (Figure 1). The ^1H NMR spectrum of Eu(DO2A2P) recorded at 274 K showed two sets of signals indicating the presence of two isomers at lower temperatures. The chemical shifts of the major component are similar to those of the Eu(DOTP) and the m isomer (TSAP) of Eu(DOTA) while the minor component appears to have chemical shifts similar to those of the M isomer (SAP) of Eu(DOTA). From the comparison of the integrals of the two sets of signals, it was estimated that under these conditions Eu(DO2A2P) exists 93% as the TSAP isomer and 7% as the SAP isomer. The ^1H NMR spectra were also recorded at 6 different temperatures from 274 to 303 K. The signals of the two isomers broaden and move closer to one other and finally the two sets of signals coalesced at 298 K (Figure S2, Supporting Information). The chemical exchange between the two isomers was also confirmed by saturation transfer experiments (Figure S3, Supporting Information). The assignment of the NMR spectra of Eu(DO2A2P) was aided by 2D NMR methods (COSY, EXSY, and HMQC). The HMQC spectrum is presented in the Supporting Information (Figure S4).

The solution structure of Lu(DO2A2P) was examined by 1D (^1H and ^{13}C) and various 2D NMR methods (COSY, EXSY, heteronuclear chemical shift correlation (HETCOR), Figures S5–S7, Supporting Information). The ^1H and ^{13}C NMR spectra (Figures 8 and 9) recorded at different temperatures revealed the presence of only the TSAP isomer. It is known from the ^1H NMR studies of Lu(DOTA) and Lu(DOTP) complexes that the ring axial protons are coupled with the geminal and vicinal axial protons, while the equatorial protons couple with the geminal protons only. Due to these couplings the axial and equatorial protons give rise to a triplet and doublet, respectively,[47] and similar couplings and multiplicities can be expected for Lu(DO2A2P). The $_1H_a-_4H_e$, $_1H_e-_4H_a$, $_2H_a-_3H_e$, and $_2H_e-_3H_a$ proton pairs of

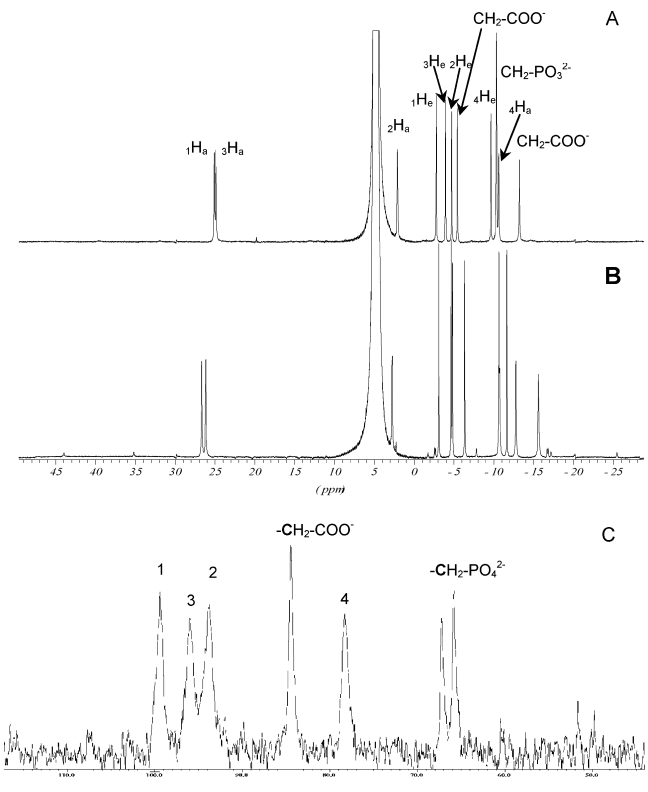

Figure 7. The ^1H and ^{13}C NMR spectra of the Eu(DO2A2P) complex. (^1H NMR spectra at 298 K (A) and 274 K (B), ^{13}C NMR spectra at 298 K(C), [EuL] = 0.04 M).

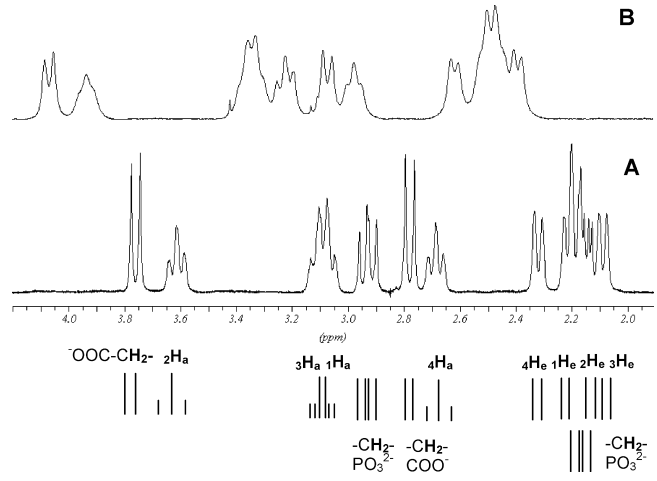

Figure 8. ^1H NMR spectra of Lu(DO2A2P) at 274 K (A) and 298 K (B) ([LuL] = 0.08 M).

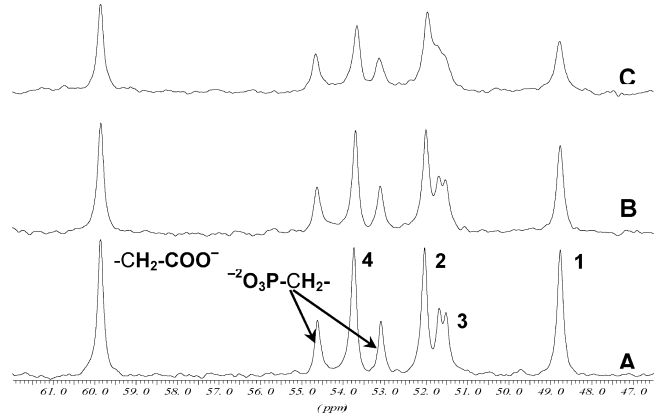

Figure 9. ^{13}C NMR spectra of Lu(DO2A2P) at 278 K (A), 288 K (B), and 298 K (C) ([LuL] = 0.08 M).

the complex exchange through fluxional motion as confirmed by the EXSY cross peaks (Figure S6, Supporting Information).

^{13}C NMR studies of Lu(DOTP) have shown that the ring carbon nuclei positioned above the plane defined by the four N atoms (e.g., 1C and 3C) are strongly coupled to the ^{31}P of the phosphonate group while coupling between the carbons located under the plane (e.g., 2C and 4C) and the ^{31}P atoms are quite weak.[16] In the ^{13}C NMR spectrum of Lu(DO2A2P), the doublet at 51.6 ppm (at 278 K) is assigned to the 3C atoms, which are coupled to the ^{31}P nuclei ($^3J_{CP} = 15.47$ Hz). At higher temperature the rate of the interconversion of the macrocyclic ring and the chemical exchange between the 3C and 2C (and between the 1C and 4C) carbons is faster. At 298 K, a broad signal appears (the signal of the 2C carbons is at 51.96 ppm). The chemical exchange process between the 1C (48.77 ppm) and 4C carbons (53.66 ppm) could directly be detected by magnetization transfer experiments (Figure S8, Supporting Information). The lower intensity signals at 53.66 and 54.66 ppm are assigned to the $-CH_2-PO_3^{2-}$ carbons, which are coupled to the ^{31}P atoms ($^1J_{CP} = 138.21$ Hz). The two doublet signals at about 3.7 and 2.7 ppm in the ^1H NMR spectrum belong to the acetate methylene protons ($^2J_{HH} = 15.95$ Hz). The protons of the $-CH_2-PO_3^{2-}$ groups appear as two double-doublets at about 2.93 and 2.17 ppm ($^2J_{HP} = 13.85$ and 16.7 Hz, respectively). The coupling constants $^3J_{HH}$, characterizing the coupling between the vicinal pairs of protons $_1H_a$–$_2H_a$ and $_3H_a$–$_4H_a$ were found to be about 13–14 Hz. The dihedral angle ϕ between these vicinal protons was estimated at ~180° from the *Karplus* equation ($^3J_{HH} = 7 - \cos\phi + 5\cos^2\phi$).[16] The ^1H and ^{13}C NMR signals of Lu(DO2A2P) broaden at higher temperatures as a result of an increased rate of enantiomerization. The rates of enantiomerization of the Lu(DOTA) and La(DOTP) complexes have been studied by NMR spectroscopy and higher activation parameters were found for the La(DOTP), which was interpreted with its more rigid structure.[16,46]

In the ^1H NMR spectra of Lu(DO2A2P), the $_4H_a$ and $_4H_e$ proton signals are well separated, so it was possible to carry out line-shape analysis by simulating the spectra gathered at different temperatures. Since the linewiths practically do not change below 272 K, the transverse relaxation time for the protons was calculated from the spectra obtained at 272 K ($T_2 = 0.07$ s). The experimental spectra were simulated using coupling constants, $^2J_{HH} = 13.45$ Hz and $^3J_{HH} = 13.6$ Hz. Examples of typical experimental and simulated spectra are shown in Figure 10. The rate constants characterizing the interconversion ($k_i = 1/\tau$) of the macrocyclic ring were calculated from the average conformation life-times (τ) (Table 5) and the activation parameters characterizing the enantiomerization process were estimated using the *Eyring* equation as $\Delta H^{\ddagger} = 60.2 \pm 3.6$ kJ mol^{-1} and $\Delta S^{\ddagger} = -14 \pm 12$ kJ mol^{-1} K^{-1}. The interconversion rate constant (k_i) at 298 K was also calculated from the selective ^{13}C magnetization transfer experiments and the $k_i = 34 \pm 3$ s^{-1} value agrees well with the data obtained from the line shape analysis (Table 5). The activation enthalpy and enthropy are similar to those reported for the La(DOTA) ($\Delta H^{\ddagger} = 59.4$ kJ mol^{-1} and $\Delta S^{\ddagger} = -4.6$ kJ mol^{-1} K^{-1}) but lower than the values ($\Delta H^{\ddagger} = 101$ kJ mol^{-1}) obtained for La(DOTP).[16,46] These data indicate that the extremely high rigidity of the macrocyclic ring in the Ln(DOTP) complexes significantly decreases if two of the phosphonates of DOTP are replaced with carboxylate groups.

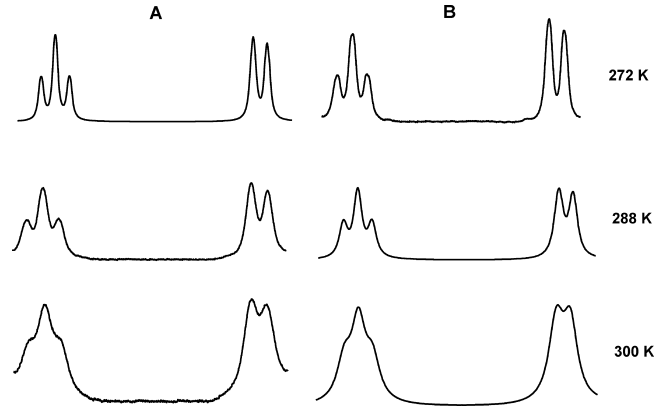

Figure 10. Experimental (A) and the simulated (B) ^1H NMR spectra of the Lu(DO2A2P).

Table 5. Rate Constants k_i (s^{-1}) Characterizing the Interconversion of the Ring of Lu(DO2A2P)

T (K)	276	282	288	294	300	306
k_i (s^{-1})	3.9	9.0	13	19	36	63

Conclusion

The cyclen based ligand, DO2A2P, was synthesized in reasonable yields. This ligand has two acetate and two methylenephosphonate pendant arms and, as expected, its protonation and chelation behavior was similar to those of DOTA and DOTP. The protonation of DO2A2P, DOTA, and DOTP is characterized by two high constants due to the protonation of two ring nitrogens. The stability constants of the DO2A2P complexes fall between those of the corresponding DOTA and DOTP complexes. The relaxivity of Gd(DO2A2P) decreases from about 4.6 to about 3.6 mM^{-1} s^{-1} between pH 2 and 7, then remains constant over the pH range 7–12. Similar to Gd(DOTP), ^{17}O NMR measurements indicate the absence of an inner-sphere water molecule. Kinetic studies on the Ce^{3+} and Gd^{3+} complexes revealed that the rate determining step in the formation of these complexes corresponds to rearrangement of a diprotonated intermediate, Ln(H_2DO2A2P)*, which occurs both spontaneously and by a OH^- assisted process. The proton assisted dissociation of Gd(DO2A2P) occurs through the diprotonated species GdH_2L both spontaneously and by a proton assisted mechanism through formation of a triprotonated species, Gd(H_3L). The order of proton assisted dissociation rates of the Gd^{3+} complexes is DOTP > DO2A2P > DOTA, which reflects the relative stability of the corresponding protonated complexes. NMR data suggest that Eu(DO2A2P) exists as 93% twisted square antiprismatic (TSAP) and 7% square antiprismatic (SAP) isomer. Activation enthalpy and entropy values for the enantiomerization process by ring interconversion suggest that Ln(DO2A2P) complexes are less rigid than the corresponding DOTP complexes

and that the rigidity of the complexes can be fine-tuned by varying the number of methylenephosphonate and acetate side arms on the ligand.

Acknowledgment. This research was supported in part by grants from the National Institutes of Health (CA-115531 and RR-02584, A.D.S.), the Robert A. Welch Foundation (AT-584, A.D.S.), OTKA K 69098 (E.B.), COST Action D-38 program (E.B.), and the EMIL Project funded by the EC FP6 Framework program (E.B.).

Supporting Information Available: Additional figures (^{17}O NMR line width data, variable temperature ^{1}H NMR studies of EuDO2A2P, ^{1}H NMR saturation transfer experiments with EuDO2A2P, HMQC spectrum of EuDO2A2P, COSY, EXSY, and HETCOR spectrum of LuDO2A2P, and magnetization transfer on the ^{13}C NMR spectra of LuDO2A2P). This material is available free of charge via the Internet at http://pubs.acs.org.

IC7024704